WORLD JOURNAL OF PHARMACY AND PHARMACEUTICAL SCIENCES
SJIF Impact Factor 7.421
Volume 7, Issue 3, 23-34 Research Article ISSN 2278 – 4357

PHYSICAL PROPERTIES AND BEHAVIORS OF MOLECULAR IMPRINTED HYDROGELS FOR CLINICAL USE

Patrick Nichols, Gerrit Winkel, Jared Bunn and Jeff Bates*

Salt Lake City USA.

Article Received on
27 December 2017,

Revised on 17 Jan. 2018,
Accepted on 07 Feb. 2018,

DOI: 10.20959/wjpps20183-10993

***Corresponding Author**
Jeff Bates
Salt Lake City USA.

ABSTRACT

Molecular imprinted hydrogels are a widely investigated means to achieve drug delivery. Much research has been done regarding the drug delivery capabilities, while much less is known about what the drug delivery process does to the hydrogel itself. We designed molecular imprinted hydrogels to mimic contact lenses for ocular drug delivery. We tested the gels to determine the longevity of use and determine if the process of delivering a drug alters the hydrogel matrix, and subsequently the drug delivery capabilities. We cycled our gels to replicate the daily use process and dehydrated them for testing. Fracture testing was performed to analyze the long term strength of each gel, and differential scanning calorimetry was done to determine any chemical deterioration due to mechanical swelling. SEM imaging was performed to visualize any microstructure alteration, and clinical aberration measurements were taken to determine any change in the index of refraction or creation of light scattering centers. Testing illustrated a long term use of no deterioration for more than 15,000 uses, with no breakdown or optical variations.

KEYWORDS: Molecular Imprinting, Drug Delivery, Hydrogel.

INTRODUCTION

Hydrogels are network polymers that are chemically linked and physically reactive to certain external stimuli.[1] Hydrophilic by nature, these matrices are capable of absorbing water and swelling to retain up to 600 times the network's weight in water.[2] The stimulus response is determined by the monomer constituents in the hydrogel network and can be controlled using molar fine-tuning.[3] This swelling reaction has led hydrogels to be an excellent candidate for biological interaction.[4] Recently there has been a great deal of effort spent on using these systems for a drug delivery system.[5] While drugs can be loaded into the mesh vacancies and

released upon swelling of the gel, more interest is in molecular imprinting to control the release kinetics of the drug.[6] Kinetics have been an issue in hydrogel drug delivery for some time, and until recently has been one of the main barriers to entering clinical usage.[7] Gels can be tailored to be very biocompatible and be very well received as a drug delivery vehicle.[8] They are a memory material[9] and thus, can be reused to provide a reliable pharmacokinetic delivery profile. While there is much interest in what the medicinal capabilities[10] imply, we aim to test the physical attributes of these systems to determine how long they can remain functional. Many hydrogels can degrade if subjected to a stress repeatedly.[11]

There has been much debate over valid testing methods, as the physical properties of hydrogels are delicate related to other biomaterials.[12] Classical testing, such as tensile or compressive testing is not performed consistently throughout the literature.[13] Some insist that testing must be done in a dehydrated state[14] to more closely model other plastic behavior, while others believe that a hydrogel needs to be tested in the same environment as it would be used and keep it well hydrated.[15] Some even postulate that constant hydration is needed for the duration of the testing process as some testing can compress the water out of the network and change properties. Our characterization methods are herein described for molecular imprinted hydrogels intended for drug delivery usage. A hydrogel is comprised of multiple components each with their own properties. Combining these monomers together during polymerization also combines the properties of each component.[16] This intrinsic summation allows for the pharmacology application we most want from a hydrogel, but many neglect the drug carrier itself.[17] We aim to provide insight into a 2-hydroxyethyl methacrylate (HEMA) based hydrogel network that has been imprinted with a prostaglandin derivative which is used to treat glaucoma.

Additionally, we were interested in the optical properties of the lenses. To be ready for clinical use, the lenses would need to be able to be transparent. The molecular imprinting process can not interfere with the light transmission or refraction, essentially not causing any aberrations in the lenses. We measured for higher order aberrations to determine lens transmittance.[18] A higher order aberration is a distortion of light caused by irregularities in the refractive index. These can originate from abnormal corneal curvature, irregularities in the crystallinity of the lens or cornea, and they are different from general disorders such as astigmatism. They are most commonly caused by a very small light scattering defects.[19]

These are typically from a non-uniform corneal curvature that causes an altered geometry. This randomness in the curve causes less than optimal transmittance and as there are common abnormalities, we measure for specific groups of shapes that scatter light in a particular way.

MATERIALS AND METHODS

The following monomers were used as received from Sigma Aldrich: 2-hydroxyethyl methacrylate (HEMA), dimethylaminoethyl methacrylate (DMA), and tetraethylene glycol dimethacrylate (TEGDMA). In addition, 2,2-Dimethoxy-2-phenylacetophenone (DMPAP), a photo initiator complex, and ethylene glycol acting as a solvent for the pregel solution, were also obtained from Sigma Aldrich. The molecular imprinted hydrogel material was synthesized by preparing a pregel solution containing the following monomers and reagents and in a molar ratio of 95 HEMA, 5 DMA, 1.5 TEGDMA for crosslinking, 5 Xalatan (Latanoprost). The pregel solution was stored at 4°C for one hour to encourage hydrogen bonding interactions prior to free radical polymerization. We then mixed these constituents in one container and placed for polymerization between 2 glass slides spaced at 400 μm apart to create a uniform thickness. The hydrogels were synthesized with UV curing by adding the ethylene glycol/drug solution to the pregel solution and polymerizing at 4°C for 2 minutes. HEMA is the backbone molecule and is responsible for both the ability of our gels to swell, along with the main portion of molecular imprinted sites.[20] Upon synthesis, the resulting material was placed in distilled water, where extraction of the template molecules occurred.

The first series of testing after polymerization was in regards to the mechanical strains of the swell/de-swell cycling. Drug delivery testing has been confirmed viable from our molecular imprinted hydrogels, but we wanted to find the endurance of these polymer networks. Each gel was subjected to a series of cycling that hydrated, and then dehydrated each gel. They were continuously exposed to this harsh succession of alternating extremes for 10, 20, and 30 days. This equates to approximately 5,200, 10,400, and 15,700 cycles. Each sample was then dehydrated to perform 3-point-bend testing in Lab VIEW. A dehydrated hydrogel can be treated as a porous solid bulk polymer and strength testing can be related to many known data.[21] From the data generated in LabVIEW a Weibull plot was created. The max load that each gel was exposed to was put in order from weakest to strongest and the distribution function F was calculated with the following formula:

$$F = \frac{i-0.3}{n+0.4} \qquad (3.1)$$

where is the rank of the failure, and n is the total number of hydrogels tested in that set. The $\ln\left(\ln\left(\frac{1}{1-F}\right)\right)$ was plotted vs the ln (σ) to generate a linear correlation between stress and failure in the Weibull plot.[22]

Next we wanted to determine if the melting or the glass transition temperature ranges had been altered by these physical strains.[23] We performed testing on samples from each group with different durations of stress exposures using Differential scanning calorimetry (DSC). DSC is a thermos-analytical technique in which the difference in the amount of heat required to increase the temperature of a sample and reference is measured as a function of temperature. Both the sample and reference are maintained at nearly the same temperature throughout the experiment. Generally, the temperature program for a DSC analysis is designed such that the sample holder temperature increases linearly as a function of time. The reference sample should have a well-defined heat capacity over the range of temperatures to be scanned. The result of a DSC experiment is a curve of heat flux versus temperature or versus time. There are two different conventions: exothermic reactions in the sample shown with a positive or negative peak, depending on the kind of technology used in the experiment. This is done by integrating the peak corresponding to a given transition. It can be shown that the enthalpy of transition can be expressed using the following equation:

$$\Delta H = KA \qquad (3.2)$$

Where H is the enthalpy of transition, K is the calorimetric constant, and A is the area under the curve. Any degradation in the polymer matrix will cause a shift in the phase transition temperature ranges.[24]

To gain a visual representation of the hydrogel matrix, we sputter coated our samples and viewed them with a Scanning Electron Microscope (SEM) to visualize any deterioration after cycling. Due to the nature of using electron waves to visualize a surface we can traditionally obtain very resolved images and generate a clear picture of the microstructure of a material.[25] In the case of polymer networks, porosity compared to a commonly imaged material is much greater, and will prove difficult to focus on a broader area. The field of view is small and we can only view the material in isolated magnification.

Finally, we used our hydrogels in a more clinical like setting. We used an OPD-Scan III Wavefront Aberrometer to collect clinically relevant data. Due to the untested physiological

interaction of our lenses we had to refrain from putting them directly into the eye, but to standardize the findings against the market ready lenses we took measurements of an eye to measure the higher order aberrations. Then in turn each lens was scanned by holding the lenses slightly away from the eye. The corneal index was measured to be 1.3375 and the wavelength of the light used in testing was 587.6 nm. The corneal measurement was for 3 mm in diameter, and the night and day setting was used.

RESULTS

To image our hydrogels we used an SEM at varying magnifications of 1,500x (A, B, C), 3,000x (D, E, F), and 15,000x (G,H,I).

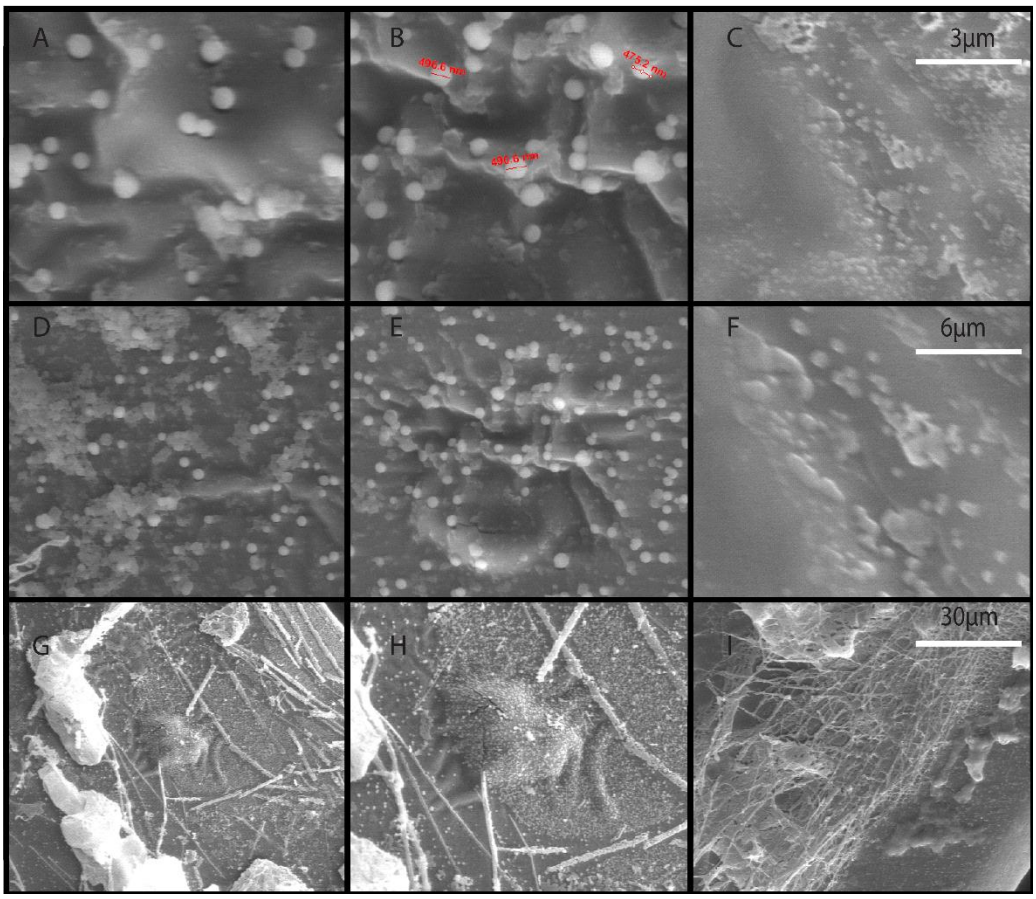

Figure 1: in the first column, (A, D, G) there are varying degrees of magnification of a molecular imprinted hydrogel. They have been made, but not released the drug for the first time yet, and have not been cycled. In the second column, (B, E, H) the same hydrogel has been redoped with drug and reimaged. The last column (C, F, I) is a control sample the was synthesized with the imprinted gels, but this gel has no drug to compare the bulk matrix with an imprinted bulk.

As you can see in image A and B, the matrix allows the drug to be imprinted and re-doped after mechanical cycling. In the images of our initial gels that were molecularly imprinted (A, D, G) you can clearly see the drug molecules randomly distributed thorough the matrix. Images of our gels after thorough cycling are shown to have full capacity of re-doping (B, E, H). The matrix has the same amount of drug molecules dispersed through the matrix, and using the non-cycled gels as a reference at each magnification you can see the matrix itself has not been degraded. The control samples were made in the same batch and were not doped with the drug to show the similarity in the hydrogel matrix, and that the molecular imprinting process does not change the bulk matrix appearance.

Then we ran our gels through a DSC to determine if the mechanical cycling was damaging. We found that all of our gels had very slight differences in T_g ranges, but none of them had any significant alterations from cycling. The T_g is a second order transition because it experiences a change in heat capacity, but does not involve latent heat. Using the software function, we were able to determine the T_g range. Each sample was found to have a glassy transition that were all nearly identical to each other. The ranges were found to have minor differences, but none were found to have been altered in a way that would negatively impact the matrix properties. Taking the median temperature from each sample we found that all had a T_g of approximately 109°**C.**

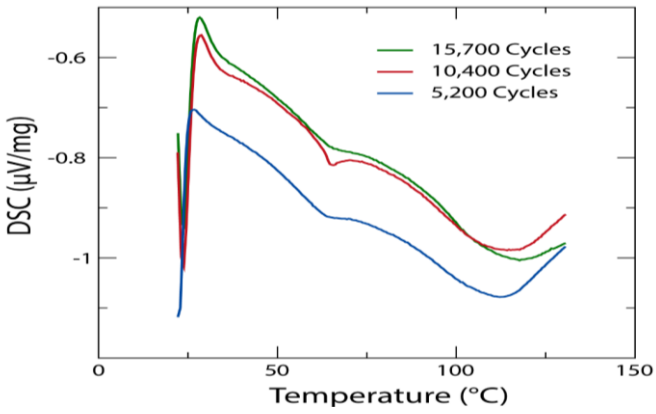

Figure 2 The green curve represents the hydrogels that have been cycled for 15,700 times, and using the DSC software determined a glass transition range of 108-109°C. The red curve illustrates the samples that have been cycled for 10,400 cycles, and using the DSC software determined a glass transition range of 108-110°C. The blue curve shows the samples that were cycled for 5,200 cycles, and using the DSC software determined a glass transition range of 108-110°C.

We also tested our gels for fracture strength and this data is presented in figure 3. Using a three point bend test we broke our samples to determine fracture strength. The Weibull analysis shows a beta parameter greater than 1 for each sample, but as the amount of cycling increases the beta parameter gets closer to 1 and the data is much more reliable. Here the Weibull analysis shows the fracture patterning with a linear regression pattern.

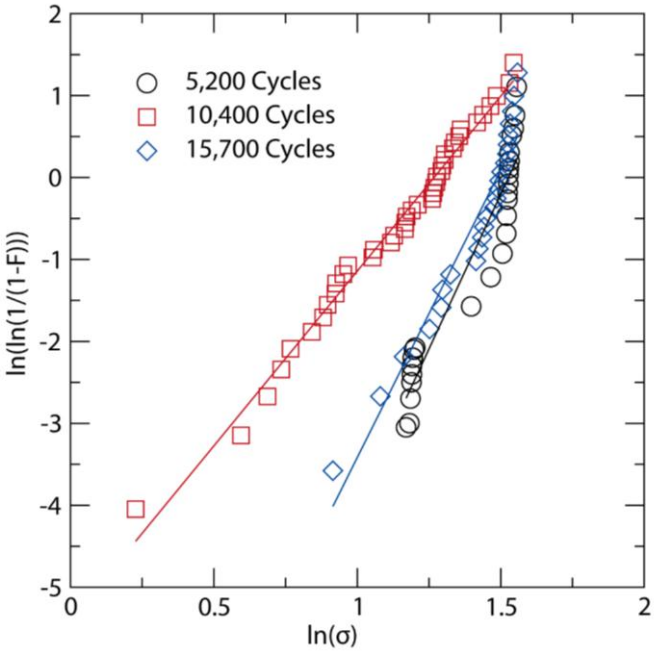

Figure 3: Fracture data is shown for samples cycled 5,200, 10,400 and 15,700 times. The linear regression for each is 7.5441x -11.52, 4.2163x-5.6309, and 7.0193x-10.434. Each R^2 value is 0.8887, 0.9854 and 0.9245.

Aberrometric measurements provide us with a comparison that gives a relevant perspective into the optical properties of our lenses and where they stand against a market ready devices. We used a clinical machine to measure the optical transmittance of our lenses and find any light scattering defects, or aberrations. Aberrations include a variety of complex geometric light scattering problems. More than just a bended lens or point defect, these aberrations cause issues with vision and are routinely measured in an eye exam.

Table 1: Aberrometric measurements were taken in a clinical setting using an OPD wavefront scanner. There were two types of measurements, an eye with and without a contact lens for a reference range, and a series of measurements holding lenses right in front of the eye. The T.Sph, T.Coma, and T.Tre columns are indicative of three prominent types of aberrations that are usually measured in a traditional eye care visit. The HO column represents the overall average higher order aberration measurements. The difference from an unimpeded eye to an eye with a lens is an order of magnitude. The lenses held in front of the eye show an increase of another order of magnitude, however still relatively small.

HOA [µm]: Cornea @ 3.00 mm -- Total Internal @ 3.00mm / Order 4				
	T. Shp	**T. Coma**	**T. Tre**	**HO**
Eye With No Lens	0.01	0.008	0.006	0.005
Eye With Acuvue Lens	0.07	0.016	0.033	0.052
Held Acuvue Lens	0.027	0.234	0.341	0.610
Held Non-Imprinted Gel	0.014	0.166	0.223	0.324
Held Imprinted Gel	0.092	0.050	0.452	0.541

The data collected in table 3.1 was to give a comparison of our lenses with market ready lenses. The eye measurement with no lens compared to a lens shows an order of magnitude HO value change. The lenses held in front of the eye show a further increase of another order of magnitude. Had the lenses all been compared on the eye, they would likely be ten times smaller in value. Our lenses show a better overall aberrometric average than the acuvue oasis name brand lenses. Each lens was held the same distance from the eye, and the measurements were taken in the same spot in the same eye. To further illustrate the difference between the inserted lens and the held lens, we have an image capture shown in figure 4 to help understanding of how the data was collected.

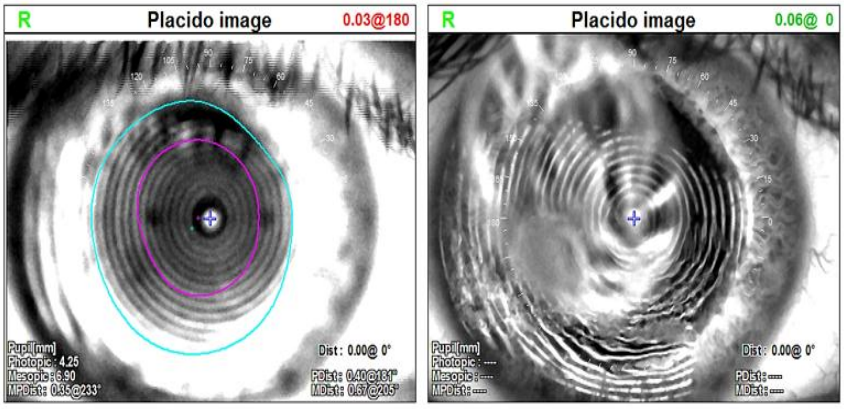

Figure 4: A side by side comparison of a lens inserted into the eye for normal wear as shown on the left, and a lens held in from of the eye as shown on the right.

The image in figure 4 shows the difference of a held lens and one that has been placed in the eye. The plus sign in the center of the pupil indicated where the aberrometric measurements were taken. The same spot in the same eye to keep a fair comparison. The lens on the right is clearly visible in from of the eye, where the lens on the left is harder to see and the software has given a general outline shown in light blue.

DISCUSSION

SEM imaging provided a great view of the hydrogel microstructure. We were clearly able to visualize the molecular imprinting as well as the bulk matrix. The drug imprinting on the matrix was unchanged from the cycling process. The gels before and after cycling had a near identical bulk matrix. The control sample showed that the imprinting process does not change the appearance of the matrix either. Due to the random nature of the polymerization process, each gel can have a slight difference in microstructure, including porosity and in turn the physical properties such as the visualization of the matrix, or the glassy transition temperature. The T_g did not change from our initial polymerized material, through the first series of cyclical swelling. The overall accumulation of physical stresses from the total cycling of 30 days did not alter the T_g. This constant T_g indicates that the swelling process does not degrade the hydrogel network for up to 15,700 cycles and this is the extreme case of full swelling due to soaking, to the drying of each lens. Each lens cycle normally consists of a slight change in water content throughout the day.

For a Weibull plot, beta is the shape parameter of the curve and is related to the slope of a linear regression probability plot. As beta is greater than 1, the reliability of fracture data decreases. However our data shows that the slope is greater than 1, but decreases over time with each series of cycling. This may be due to the fact that the polymerization process is never 100 percent and there are always some amount of unreacted monomer. As the bulk material cycles, the amount of these unreacted monomers decreases as they are mechanically expelled over time from the number of swelling sequences. These monomers could be skewing the fracture data and the more they are removed from the bulk, the more reliable the data becomes. This is illustrated by the increase of the R^2 number that connects the data to the linear regression line. The position parameter gamma decreases over the course of the swelling cycle. This correlates to the same vacancy formation from the escaping monomers. This could imply that the monomers in the bulk could help absorb some of the physical stress and increase fracture toughness. This shift in the gamma value numerically indicates that the

gels begin fracturing sooner, but the data on the plot suggest that the bulk of the gels still fracture at higher stress loads. Similarly, the lack of change in the DSC curves suggest that the unreacted monomers are not contributing a significant amount to the bulk material characteristics and their contribution to the T_g and melting temperatures are negligible.

The aberrometry measurements illustrate a clear lens that will not cause any significant transmittance issues. The measurements actually indicate a better transmittance with fewer scattering events than a clinical lens. Much more data will need to be collected in a more controlled setting to further prove this improved difference, but these initial findings show that our lenses could be used without fear of optical issues.

CONCLUSION

The determination of molecular imprinted polymers as viable drug delivery systems is dependent on the reversible swelling action and the load-release mechanism of the drug. The aim of this paper was to evaluate the reliability and stability of these hydrogels during the delivery process over time. Our results indicate that the gels remain stable with up to 15,700 uses. As illustrated by the Weibull analysis, the physical strength is reliable for the lifetime of the gels despite the rigorous mechanical cycling. The DSC data supports the fracture analysis and also indicates there was no chemical breakdown as the T_g remains unchanged. This is all visualized in the SEM images where the gel matrix is not deteriorated and the drug loading capacity is equivalent before and after cycling. These data provide strong evidence that molecular imprinted hydrogels will be able to last far longer than is advisable to continue wearing contact lenses.

ACKNOWLEDGEMENTS

Thanks to the University of Utah for providing assistance in collecting the data, also to the department of Materials Science and Engineering. They provided the LabVIEW kit to allow for the fracture testing of the hydrogel samples.

REFERENCES

1. C. Alexander, Stimuli-responsive hydrogels: Drugs take control, Nature materials, 2008; 7(10): 767-768.
2. F. Hua, M. Qian, Synthesis of self-crosslinking sodium polyacrylate hydrogel and water-absorbing mechanism, Journal of materials science, 2001; 36(3): 731-738.

3. K.S. Soppimath, T.M. Aminabhavi, A.M. Dave, S.G. Kumbar, W. Rudzinski, Stimulus-responsive "smart" hydrogels as novel drug delivery systems, Drug development and industrial pharmacy, 2002; 28(8): 957-974.
4. G. Chan, D.J. Mooney, New materials for tissue engineering: towards greater control over the biological response, Trends in biotechnology, 2008; 26(7): 382-392.
5. B. Jeong, A. Gutowska, Lessons from nature: stimuli-responsive polymers and their biomedical applications, Trends in biotechnology, 2002; 20(7): 305-311.
6. P. Gupta, K. Vermani, S. Garg, Hydrogels from controlled release to pH-responsive drug delivery, Drug discovery today, 2002; 7(10): 569-579.
7. H. Hiratani, Y. Mizutani, C. Alvarez-Lorenzo, Controlling drug release from imprinted hydrogels by modifying the characteristics of the imprinted cavities, Macromolecular bioscience, 2005; 5(8): 728-733.
8. T.R. Hoare, D.S. Kohane, Hydrogels in drug delivery: progress and challenges, Polymer, 2008; 49(8): 1993-2007.
9. C. Liu, H. Qin, P. Mather, Review of progress in shape-memory polymers, Journal of Materials Chemistry, 2007; 17(16): 1543-1558.
10. R. Langer, D.A. Tirrell, Designing materials for biology and medicine, Nature, 2004; 428(6982): 487-492.
11. M.J. Whitcombe, N. Kirsch, I.A. Nicholls, Molecular imprinting science and technology: a survey of the literature for the years 2004–2011, Journal of Molecular Recognition, 2014; 27(6): 297-401.
12. K.S. Anseth, C.N. Bowman, L. Brannon-Peppas, Mechanical properties of hydrogels and their experimental determination, Biomaterials, 1996; 17(17): 1647-1657.
13. V. Normand, D.L. Lootens, E. Amici, K.P. Plucknett, P. Aymard, New insight into agarose gel mechanical properties, Biomacromolecules, 2000; 1(4): 730-738.
14. M. Oyen, Mechanical characterisation of hydrogel materials, International Materials Reviews, 2014; 59(1): 44-59.
15. E.M. Ahmed, Hydrogel: Preparation, characterization, and applications: A review, Journal of advanced research, 2015; 6(2): 105-121.
16. A. Richter, G. Paschew, S. Klatt, J. Lienig, K.-F. Arndt, H.-J.P. Adler, Review on hydrogel-based pH sensors and microsensors, Sensors, 2008; 8(1): 561-581.
17. B. Singh, N. Chauhan, V. Sharma, Design of molecular imprinted hydrogels for controlled release of cisplatin: Evaluation of network density of hydrogels, Industrial & Engineering Chemistry Researchm 2011; 50(24): 13742-13751.

18. J. He, S. Marcos, R. Webb, S. Burns, Measurement of the wave-front aberration of the eye by a fast psychophysical procedure, JOSA A, 1998; 15(9): 2449-2456.
19. S.C. Schallhorn, A.A. Farjo, D. Huang, B.S.B. Wachler, W.B. Trattler, D.J. Tanzer, P.A. Majmudar, A. Sugar, Wavefront-guided LASIK for the correction of primary myopia and astigmatism: a report by the American Academy of Ophthalmology, Ophthalmology, 2008; 115(7): 1249-1261.
20. K. Sreenivasan, R. Sivakumar, Imparting recognition sites in poly (HEMA) for two compounds through molecular imprinting, Journal of applied polymer science, 1999; 71(11): 1823-1826.
21. N. Annabi, J.W. Nichol, X. Zhong, C. Ji, S. Koshy, A. Khademhosseini, F. Dehghani, Controlling the porosity and microarchitecture of hydrogels for tissue engineering, Tissue Engineering Part B: Reviews, 2010; 16(4): 371-383.
22. T. Nakajima, Y. Fukuda, T. Kurokawa, T. Sakai, U.-i. Chung, J.P. Gong, Synthesis and fracture process analysis of double network hydrogels with a well-defined first network, ACS Macro Letters, 2013; 2(6): 518-521.
23. J. Maitra, V.K. Shukla, Cross-linking in hydrogels-a review, American Journal of Polymer Science, 2014; 4(2): 25-31.
24. Y. Liu, B. Bhandari, W. Zhou, Study of glass transition and enthalpy relaxation of mixtures of amorphous sucrose and amorphous tapioca starch syrup solid by differential scanning calorimetry (DSC), Journal of food engineering, 2007; 81(3): 599-610.
25. Y. Luo, K.R. Kirker, G. D. Prestwich, Cross-linked hyaluronic acid hydrogel films: new biomaterials for drug delivery, Journal of controlled release, 2000; 69(1): 169-184.